

Superconducting Phase with the $(d + id)$ Order Parameter in an Ensemble of Hubbard Fermions on the Triangular Lattice

V. V. Val'kov^{a, *}, T. A. Val'kova^b, and V. A. Mitskan^{a, c}

^a Kirensky Institute of Physics, Siberian Branch, Russian Academy of Sciences, Akademgorodok, Krasnoyarsk, 660036 Russia

^b Siberian Federal University, Krasnoyarsk, 660041 Russia

^c Reshetnev Siberian State Aerospace University, Krasnoyarsk, 660014 Russia

* e-mail: vvv@iph.krasn.ru

Received July 7, 2015; in final form, August 5, 2015

In the framework of the $t-J_1-J_2-V$ model, the integral equation determining the order parameter $\Delta(p)$ of the superconducting phase is derived for an ensemble of strongly correlated fermions on a triangular lattice using the diagram technique for the Hubbard operators. Taking into account the interaction between the Hubbard fermions within two coordination spheres, we demonstrate that the exact analytical solution $\Delta_2(p)$ of this equation for the superconducting phase with the $(d_{x^2-y^2} + id_{xy})$ symmetry can be expressed as a superposition of two chiral basis functions. This gives rise to a new set of nodal points for the complex parameter $\Delta_2(p)$. Moreover, at some critical value x_c of the charge carrier density, we obtain a gapless phase with six Dirac points. The passing of x through $x = x_c$ is accompanied by the topological quantum transition corresponding to the change in the topological parameter Q .

DOI: 10.1134/S0021364015180162

1. INTRODUCTION

The discovery of superconductivity with $T_c = 5$ K in water-intercalated $\text{Na}_x\text{CoO}_2 \cdot y\text{H}_2\text{O}$ sodium cobaltite ($x \simeq 0.3$) [1] initiated a considerable interest in studies of this novel class of layered materials with a triangular lattice. First, the problem concerning the nature of the superconducting pairing appeared. The data on the spin–lattice relaxation rate at $T = T_c$ suggested the existence of the anisotropic superconducting order parameter and an unconventional nature of the superconducting pairing [2]. Similar results were provided by the muon spectroscopy [3] and by the specific heat measurements [4]. After that, the problem on the symmetry of the superconducting order parameter became quite challenging. The studies performed using high-quality $\text{Na}_x\text{CoO}_2 \cdot y\text{H}_2\text{O}$ single crystals [5] demonstrated a decrease in the spin contribution to the Knight shift on cooling below T_c , which could indicate the spin-singlet superconductivity. Moreover, this suggested the existence of antiferromagnetic correlations.

A significant interest in the fermion systems on the triangular lattice is also related to the possible existence of the superconducting order parameter with the $(d_{x^2-y^2} + id_{xy})$ type of symmetry. Such a superconducting state with broken time reversal symmetry was stud-

ied earlier for the $t-J$ model in the framework of the mean-field description of the state of resonance valence bonds [6, 7]. It was also considered based on the variational approach for the Gutzwiller approximation [8] and was discussed in the framework of the slave-boson approximation [9]. These studies involved the suggestion that the interaction between fermions occurs only within the first coordination sphere. Then, the nodal points for the chiral $\Delta_2(p)$ parameter are located only at the center and boundaries of the Brillouin zone. Therefore, the chiral $d + id$ superconducting phase remains gapped at all admissible doping levels. However, this contradicts the available NMR data [2].

A way for overcoming this discrepancy was suggested in [10]. The authors of that work argue that only involving the pairings of electrons located at the next-nearest-neighbor sites can give rise to the nodal points of the complex order parameter $\Delta_2(p)$ appearing inside the Brillouin zone. This important result means that, at a certain electron density, when the Fermi surface intersects the set of zeros of $\Delta_2(p)$, the spectrum of the fermion excitations in the superconducting phase is characterized by six Dirac points. At the same time, the superconducting phase becomes gapless. This is in agreement with the experimental data [2].

The importance of the conclusion on the existence of Dirac points in the superconducting phase is also related to the increasing activity in the studies concerning the possibility of observing Majorana fermions in spin-singlet superconductors with the spectrum containing nodes [11].

In this connection, the existence of the nodal points of $\Delta_2(p)$ within the Brillouin zone owing to the pairing strictly for the second coordination sphere, whereas the similar coupling is absent for the nearest neighbors, seems to be quite artificial. If the system exhibits the couplings both in the first and second coordination spheres, the superconducting phase for which the $\Delta_2(p)$ parameter is determined only by the basis functions related to the second coordination sphere does not meet the necessary conditions of self-consistency. This is the main problem. In this work, we propose a solution to this problem in the framework of the $t-J_1-J_2-V$ model on the triangular lattice. This model takes into account the exchange interaction between the neighbor sites within two coordination spheres, as well as the charge fluctuations for the nearest-neighbor ions.

2. HAMILTONIAN AND GREEN'S FUNCTIONS IN THE ATOMIC REPRESENTATION

We describe an ensemble of Hubbard fermions within the $t-J_1-J_2-V$ model

$$H = \sum_{f\sigma} (\varepsilon - \mu) X_f^{\sigma\sigma} + \sum_f (2\varepsilon + U - 2\mu) X_f^{22} + \sum_{fm\sigma} t_{fm} X_f^{2\bar{\sigma}} X_m^{\bar{\sigma}2} + \sum_{fm\sigma} J_{fm} (X_f^{\uparrow\downarrow} X_m^{\downarrow\uparrow} - X_f^{\uparrow\uparrow} X_m^{\downarrow\downarrow}) + \frac{1}{2} \sum_{f\delta} V (\hat{n}_f - \langle \hat{n}_f \rangle) \cdot (\hat{n}_{f+\delta} - \langle \hat{n}_{f+\delta} \rangle). \quad (1)$$

The first two terms of this Hamiltonian describe the one- and two-electron states at the sites of the triangular lattice in terms of the Hubbard operators in the atomic representation [12, 13]. Here, ε is the energy of the one-electron state, μ is the chemical potential of the ensemble, and U is the Hubbard repulsion energy. The off-diagonal Hubbard operators describe the transitions between the one-site states. The third term in the Hamiltonian corresponds to the process where the transition from the state with two electrons to the one-electron state with the spin projection $\bar{\sigma}$ (annihilation of an electron with the spin projection σ) occurs at the m th site and the transition from the one-electron state $|\bar{\sigma}\rangle$ to the state with two electrons $|2\rangle$ accompanies the creation of an electron with the same spin projection at the f th site. The probability amplitude for such electron hopping is determined by the parameter t_{fm} . The fourth term in the Hamiltonian corresponds to the exchange interaction in the $t-J$ model in

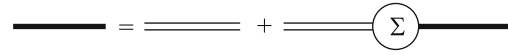


Fig. 1. Diagrammatic representation of the Dyson equation for the Hubbard fermions. The double line denotes the Green's function corresponding to the collective excitations.

the representation of Hubbard operators [14]. Here, J_{fm} is the exchange integral describing the coupling of ions in the one-electron states at the f and m sites. The last term in the Hamiltonian accounts for the existence of charge fluctuations in the system. These fluctuations arise owing to the Coulomb repulsion between electrons located at the nearest-neighbor sites (δ is the vector connecting the nearest neighbors). Here, V is the parameter characterizing the magnitude of such correlations. The operator describing the number of electrons at site f is given by the expression $\hat{n}_f = X_f^{\uparrow\uparrow} + X_f^{\downarrow\downarrow} + 2X_f^{22}$.

To describe the superconducting phase, we use the diagram technique for the Hubbard operators [13]. We introduce the normal and anomalous Matsubara Green's functions in the atomic representation

$$D_{\alpha\beta}(f\tau, m\tau') = -\langle T_\tau X_f^\alpha(\tau) X_m^\beta(\tau') \rangle = \frac{T}{N} \sum_{p, \omega_n} \exp\{ip(f-m) - i\omega_n(\tau - \tau')\} D_{\alpha\beta}(p, i\omega_n).$$

To contract the expression below, we compose the matrix Green's function

$$\hat{D}(p, i\omega_n) = \begin{pmatrix} D_{\downarrow 2, \downarrow 2}(p, i\omega_n) & D_{\downarrow 2, \uparrow 2}(p, i\omega_n) \\ D_{\uparrow 2, \downarrow 2}(p, i\omega_n) & D_{\uparrow 2, \uparrow 2}(p, i\omega_n) \end{pmatrix},$$

and take into account that this function is related to the function $\hat{G}(p, i\omega_n)$ and the force operator $\hat{P}(p, i\omega_n)$ by the formula $\hat{D}(p, i\omega_n) = \hat{G}(p, i\omega_n) \cdot \hat{P}(p, i\omega_n)$.

The Dyson equation for the function $\hat{G}(p, i\omega_n)$ in graphical form is shown in Fig. 1.

After putting the analytical expressions into correspondence with the graphical elements, we obtain

$$\hat{G} = \frac{1}{\det(p, i\omega_n)} \begin{pmatrix} i\omega_n + \xi_p + \Sigma & \Delta(p, i\omega_n) \\ \Delta^*(p, i\omega_n) & i\omega_n - \xi_p - \Sigma \end{pmatrix},$$

where

$$\det(p, i\omega_n) = (i\omega_n - \xi_p - \Sigma) \times (i\omega_n + \xi_p + \Sigma) - |\Delta(p, i\omega_n)|^2.$$

Here, we take into account that the matrix of the mass operator is defined as

$$\hat{\Sigma}(p, i\omega_n) = \begin{pmatrix} \Sigma(p, i\omega_n) & \Delta(p, i\omega_n) \\ \Delta^*(p, i\omega_n) & \Sigma(p, i\omega_n) \end{pmatrix},$$

and two thin lines correspond to the cooperative function for the Hubbard fermions in the loopless approximation

$$\hat{G}^{(0)}(p, i\omega_n) = \begin{pmatrix} 1/(i\omega_n - \xi_p) & 0 \\ 0 & 1/(i\omega_n + \xi_p) \end{pmatrix},$$

where $\xi_p = \varepsilon + N_{2\sigma}t_p$ is the μ spectrum of the Hubbard fermions, $N_{2\sigma} = N_2 + N_\sigma$ is the well-known Hubbard renormalization factor, and N_2 and N_σ are the occupation numbers of the one-site states with two electrons and with one electron with the spin projection σ , respectively.

3. SELF-CONSISTENT EQUATION FOR THE SUPERCONDUCTING ORDER PARAMETER

Further, we limit ourselves to the study of the characteristic features of the superconducting phase with the $(d + id)$ symmetry of the order parameter. For this reason, we consider only such contributions to the mass operator that are responsible for the formation of this phase. Accordingly, we shall not represent the diagrams contributing to the anomalous components of the mass operator, which are related to the kinematic interaction of the Hubbard fermions [13]. Then, in the mean-field approximation, the anomalous components of the mass operator should be determined by three diagrams. Two upper diagrams in Fig. 2 describe the contribution of the exchange interaction (the wavy line) to the anomalous mass operator, whereas the lower diagram is related to the Coulomb interaction (the dashed line). The indices near the lines corresponding to the Green's functions specify the root vectors [12]. Putting the analytical expressions into correspondence with these figures, we find

$$\Delta(p) = \frac{T}{N} \sum_{q, \omega_m} \{ J_{p-q} [G_{\uparrow 2, 2\downarrow}(q, i\omega_m) - G_{\downarrow 2, 2\uparrow}(q, i\omega_m)] + V_{p-q} G_{\downarrow 2, 2\uparrow}(q, i\omega_m) \}. \quad (2)$$

Using the expression for the matrix Green's function $\hat{G}(q, i\omega_m)$, we obtain the following self-consistent equation for the superconducting order parameter after the summation over the Matsubara frequencies

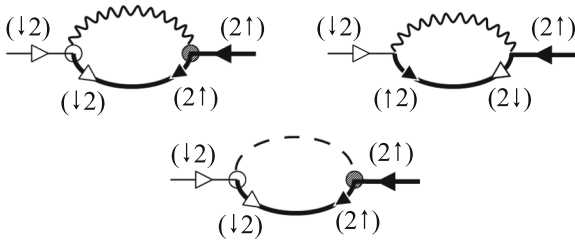


Fig. 2. One-loop diagrams for the mass operator.

and taking into account the properties of the Green's functions:

$$\Delta(p) = \frac{1}{N} \sum_q (J_{p+q} + J_{p-q} - V_{p-q}) \times \Delta(q) \frac{\tanh(E_q/2T)}{2E_q},$$

where $E_q = \sqrt{\xi_q^2 + |\Delta(q)|^2}$ is the excitation spectrum of the superconducting phase.

4. CHIRAL $d + id$ SUPERCONDUCTING PHASE

For the triangular lattice, the terms in the kernel of the integral equation have the form

$$\begin{aligned} J_q &= 2J_1 \left[\cos(q_y) + 2 \cos\left(\frac{\sqrt{3}q_x}{2}\right) \cos\left(\frac{q_y}{2}\right) \right] \\ &+ 2J_2 \left[\cos(\sqrt{3}q_x) + 2 \cos\left(\frac{\sqrt{3}q_x}{2}\right) \cos\left(\frac{3q_y}{2}\right) \right], \quad (3) \\ V_q &= 2V \left[\cos(q_y) + 2 \cos\left(\frac{\sqrt{3}q_x}{2}\right) \cos\left(\frac{q_y}{2}\right) \right]. \end{aligned}$$

It is easy to check that the solution of the equation for the superconducting gap with the $d + id$ symmetry (with the orbital angular momentum $l = 2$) can be written in the form of the superposition

$$\Delta_2(q) = 2\Delta_{21}^0 \varphi_{21}(q) + 2\Delta_{22}^0 \varphi_{22}(q), \quad (4)$$

where the chiral basis functions

$$\begin{aligned} \varphi_{21}(q) &= \cos q_y - \cos\left(\frac{\sqrt{3}q_x}{2}\right) \cos\left(\frac{q_y}{2}\right) \\ &+ i\sqrt{3} \sin\left(\frac{\sqrt{3}q_x}{2}\right) \sin\left(\frac{q_y}{2}\right), \\ \varphi_{22}(q) &= \cos \sqrt{3}q_x - \cos\left(\frac{\sqrt{3}q_x}{2}\right) \cos\left(\frac{3q_y}{2}\right) \\ &- i\sqrt{3} \sin\left(\frac{\sqrt{3}q_x}{2}\right) \sin\left(\frac{3q_y}{2}\right) \end{aligned} \quad (5)$$

correspond to the first and second coordination spheres [10].

Substituting (4) into the equation for the superconducting gap, we obtain a set of two algebraic equations for the amplitudes

$$\begin{aligned} (1 - A_{11})\Delta_{21}^0 - A_{12}\Delta_{22}^0 &= 0, \\ -A_{21}\Delta_{21}^0 + (1 - A_{22})\Delta_{22}^0 &= 0. \end{aligned} \quad (6)$$

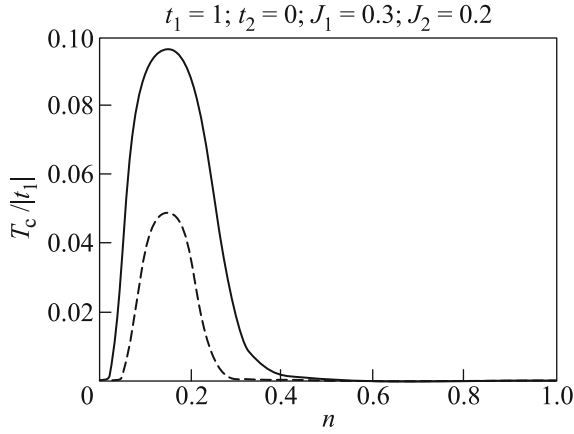


Fig. 3. Critical temperature of the transition to the superconducting phase versus the electron density at $V =$ (solid line) 0 and (dashed line) 0.3.

Functions A_{ij} involved in these equations are given by the expressions

$$\begin{aligned}
 A_{11} &= (2J_1 - V) \frac{1}{N} \sum_q \cos\left(\frac{\sqrt{3}}{2}q_x + \frac{1}{2}q_y\right) \\
 &\quad \times \left[\cos\left(\frac{\sqrt{3}}{2}q_x + \frac{1}{2}q_y\right) - \cos q_y \right] L_q, \\
 A_{12} &= (2J_1 - V) \frac{1}{N} \sum_q \cos\left(\frac{\sqrt{3}}{2}q_x + \frac{1}{2}q_y\right) \\
 &\quad \times \left[\cos\left(\frac{\sqrt{3}}{2}q_x - \frac{3}{2}q_y\right) - \cos\sqrt{3}q_x \right] L_q, \\
 A_{22} &= 2J_2 \frac{1}{N} \sum_q \cos(\sqrt{3}q_x) \\
 &\quad \times \left[\cos(\sqrt{3}q_x) - \cos\left(\frac{\sqrt{3}}{2}q_x + \frac{3}{2}q_y\right) \right] L_q, \\
 A_{21} &= 2J_2 \frac{1}{N} \sum_q \cos(\sqrt{3}q_x) \\
 &\quad \times \left[\cos q_y - \cos\left(\frac{\sqrt{3}}{2}q_x + \frac{1}{2}q_y\right) \right] L_q,
 \end{aligned} \tag{7}$$

where $L_q = \tanh(E_q/2T)/E_q$.

The set of equations (6) describes the temperature dependence of $\Delta_2(q)$. The ordering temperature T_c is determined by the existence at $\Delta_2(q) = 0$ of a nontrivial solution of the equation

$$(1 - A_{11})(1 - A_{22}) - A_{12}A_{21} = 0. \tag{8}$$

In Fig. 3, we illustrate the effect of the Coulomb correlations on the electron density dependence of temperature of the transition to the superconducting phase with the $d + id$ symmetry. The Coulomb interaction leads to the enhancement of the relative contribution of the second basis function. Owing to that, the

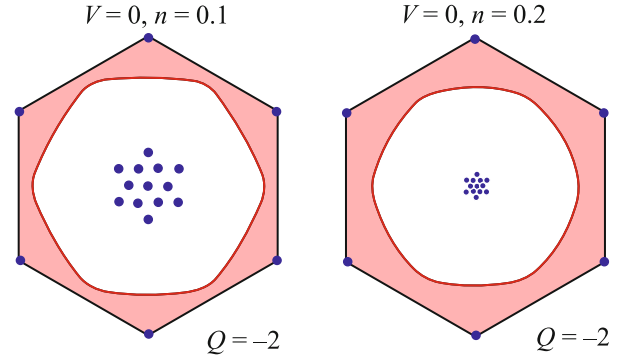


Fig. 4. (Color online) Nodal points for $\Delta_2(q)$ and the Fermi contour disregarding intersite correlations. With the growth of the density of Hubbard fermions, the set of nodal points moves faster than the Fermi contour, and hence the quantum topological transition does not take place. The used values of the parameters (in units of $|t_1|$) are $J_1 = 0.3$, $J_2 = 0.2$, and $t_2 = t_3 = 0$.

transition to the superconducting phase does not disappear in spite of the suppressed tendency to the Cooper pairing, which is due only to the exchange interaction within the first coordination sphere.

5. EFFECT OF THE COULOMB CORRELATIONS ON THE EVOLUTION OF THE NODAL POINTS

The importance of involving the Coulomb correlations is related, in particular, to the additional possibility of inducing the quantum topological transition by an increase in the charge carrier density. It is well known that the changes in the topological characteristics of the superconducting phase with the complex order parameter $\Delta_2(q) = \text{Re}\Delta_2(q) + i\text{Im}\Delta_2(q)$ occur when the Fermi surface crosses the nodal points of $\Delta_2(q)$. The existence of the real and imaginary parts makes it more difficult to meet this condition. As is shown in [10], the existence of a single basis function corresponding to the second coordination sphere leads to zeros of $\Delta_2(q)$ located inside the Brillouin zone.

The inclusion of the interactions from two coordination spheres can change the situation qualitatively because the positions of zeros in the case of two basis functions depend on the ratio of the amplitudes Δ_{21}^0 and Δ_{22}^0 of the complex order parameter $\Delta_2(q) = 2\Delta_{21}^0\phi_{21}(q) + 2\Delta_{22}^0\phi_{22}(q)$. In this case, the “old” zeros can disappear and the new ones with the positions strongly dependent on the system parameter can arise. Such a situation is demonstrated below. In Fig. 4, we show the positions of the nodal points of $\Delta_2(q)$ within the Brillouin zone and the Fermi contour at two values of the electron density n in the case where the intersite Coulomb interactions are neglected. The growth of n

results in changes in the $\Delta_{21}^0/\Delta_{22}^0$ ratio. This leads to the displacement of nodal points toward the center of the Brillouin zone. This displacement is more pronounced than that of the Fermi contour. As a result, the change in the fermion density in this regime should not be accompanied by the topological phase transition. This is a manifestation of one of the significant features related to the superposition type of the chiral order parameter. Let us recall that the nodal points when $\Delta_2(q) = 2\Delta_{22}^0\Phi_{22}(q)$ do not move and the Fermi contour crosses these points with the growth of n and this crossing is accompanied by the topological phase transition.

When Coulomb correlations are taken into account, the situation can change drastically. In particular, there is a range of parameters ($V \sim J_1$) within which an interplay of the nodal points and the Fermi contour changes qualitatively (see Fig. 5). In this case, the displacement of nodal points is relatively slow and the Fermi contour has time to “overtake” them. At the critical value of the charge carrier density, the set of nodal points of $\Delta_2(q)$ is located at the Fermi contour. Thus, the Coulomb correlations between the Hubbard fermions from the first coordination sphere not only suppress the tendency to the pairing but, modifying the partial amplitudes $\Delta_{21}^0\Phi_{21}(q)$ and $\Delta_{22}^0\Phi_{22}(q)$, can significantly affect the dynamics of nodal points, thus initiating the quantum topological transition in the superconducting state.

When $V \gg J_1$, the set of nodal points becomes closer to that determined only by the second basis function. Moreover, the behavior of the system with the variation of the charge carrier density corresponds to the scenario described in [10] and the enhancement of the Coulomb interaction manifests itself only as the lowering of the superconducting transition temperature.

6. QUANTUM TOPOLOGICAL TRANSITION IN THE SUPERCONDUCTING PHASE WITH THE SUPERPOSITION-TYPE CHIRAL $d + id$ ORDER PARAMETER

The complex form of the chiral $d_{x^2-y^2} + id_{xy}$ superconducting order parameter $\Delta_2(q)$ manifests itself in the topological features of the superconducting phase. The introduction of the unit vector $\mathbf{m} = \{m_x, m_y, m_z\}$ [16] with the components

$$m_x = \frac{\text{Re } \Delta_2(q)}{E_q}, \quad m_y = \frac{-\text{Im } \Delta_2(q)}{E_q}, \quad m_z = \frac{\xi_q}{E_q}$$

makes it possible to find the correspondence between the points of the Brillouin zone and those of the unit sphere. Then, the motion over the Brillouin zone is put into correspondence with the motion over the unit

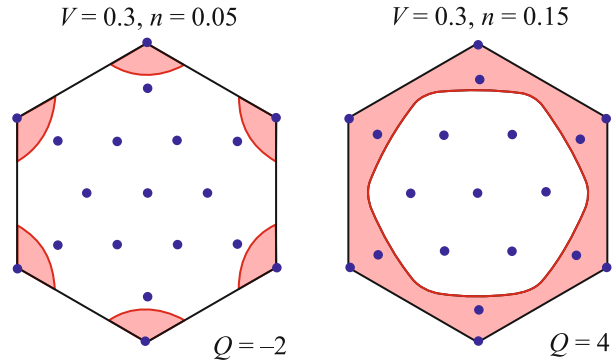


Fig. 5. (Color online) Nodal points for $\Delta_2(q)$ and the Fermi contour with the inclusion of intersite correlations. With the growth of the density of Hubbard fermions, the Fermi contour moves faster than the nodal points are displaced. The quantum topological transition occurs in the superconductor. The used values of the parameters (in units of $|t_1|$) are $J_1 = 0.3$, $J_2 = 0.2$, and $t_2 = t_3 = 0$.

sphere. To identify different classes of such trajectories, the topological index is usually introduced [10]

$$Q = \frac{1}{8\pi} \sum_{\Delta} \mathbf{m}_1 \cdot [\mathbf{m}_2 \times \mathbf{m}_3],$$

where summation is performed over all triangular plaquettes and the vectors \mathbf{m}_1 , \mathbf{m}_2 , and \mathbf{m}_3 are calculated at the apexes of such plaquettes. The value of Q characterizes the topological structure of the superconducting phase. It is related to the arrangement of the nodal points of $\Delta_2(q)$. If the changes in the charge carrier density lead to the intersection of the Fermi contour of the normal phase with the nodal points, the topological quantum transition occurs. In our case

where $\Delta_2(q) = 2\Delta_{21}^0\Phi_{21}(q) + 2\Delta_{22}^0\Phi_{22}(q)$, such transition may be initiated by the Coulomb interaction. In Fig. 4, we can see that the growth of the charge carrier density in the absence of the Coulomb interaction is not accompanied by any changes in the topological parameter $Q = -2$. If the Coulomb interaction is taken into account, then (as we can see in Fig. 5) the Fermi contour of the normal phase intersects the set of nodal points of $\Delta_2(q)$ at some critical value of the charge carrier density and the topological transition takes place. At the critical charge carrier density, the topological parameter changes from $Q = -2$ to $+4$.

7. CONCLUSIONS

The main results of our work can be summarized as follows.

(i) Using the diagram technique for Hubbard operators and taking into account the interactions of electrons within two coordination spheres for the triangular lattice, we have obtained the integral equation determining the order parameter for the superconducting phase.

(ii) It has been shown that the exact solution of this equation in the $d + id$ channel is determined by a linear superposition of two chiral basis functions $\varphi_{21}(q)$ and $\varphi_{22}(q)$: $\Delta_2(q) = 2\Delta_{21}^0\varphi_{21}(q) + 2\Delta_{22}^0\varphi_{22}(q)$.

(iii) For the system of Hubbard fermions interacting at the nearest- and next-nearest-neighbor sites, the formation of the set of nodal points for the chiral order parameter $\Delta_2(q)$ can occur according to two qualitatively different scenarios.

In the first scenario, the set of nodal points $\{q_\alpha\}$ is determined only by the first (second) chiral basis function and is displaced only slightly after the inclusion of the second (first) basis function. This occurs, for example, if the interaction with the nearest fermions is taken into account at a fixed interaction with the next-nearest neighbors. If the pairing potential of such interaction is substantially weakened by the Coulomb repulsion of electrons from the sphere of the nearest neighbors, the amplitude Δ_{21}^0 can be small and the nodal points of the order parameter $\Delta_2(q)$ could be close to those of the basis function $\varphi_{22}(q)$. Just this case was discussed in [10].

A qualitatively different scenario for arising nodal points $\{q_\alpha\}$ of the chiral order parameter $\Delta_2(q)$ takes place when the basis functions $\varphi_{21}(q_\alpha)$ and $\varphi_{22}(q_\alpha)$ at the points $\{q_\alpha\}$ are about unity rather than zero. Then, the new set of nodal points appear as the superposition $\Delta_2(q) = 2\Delta_{21}^0\varphi_{21}(q) + 2\Delta_{22}^0\varphi_{22}(q)$ and a nonzero value of $\Delta_{21}^0\varphi_{21}(q_\alpha)$ is compensated by a nonzero value of $\Delta_{22}^0\varphi_{22}(q_\alpha)$. It is essential that the set of nodal points $\{q_\alpha\}$ obtained in such a way strongly depends on the ratio of the amplitudes Δ_{21}^0 and Δ_{22}^0 . Since these amplitudes are determined from the solution of the self-consistent equations, the location of $\{q_\alpha\}$ in the Brillouin zone will appreciably vary with changes in the parameters characterizing the interactions, the density of Hubbard fermions, and generally the temperature. From the above discussion, it follows that the new set of nodal points $\{q_\alpha\}$ should exhibit a pronounced dynamics (within the first scenario, the nodal points are nearly immovable) with the change, for example, in the density of Hubbard fermions. Such a behavior is illustrated in the figures presented above, which demonstrate this dynamic feature.

(iv) With the variation of doping at the point $x = x_c$ when the Fermi contour crosses the new set of nodal points $\{q_\alpha\}$, the superconductor exhibits the topological quantum transition at which the topological parameter Q changes -2 to $+4$.

(v) The revealed features of the charge carrier dependence of the new set of the nodal points are essential for finding the conditions of the implementation of the Majorana fermions. The location of the nodal points for the chiral order parameter on the Fermi surface of the normal phase at some critical doping level x_c leads to the formation of the gapless superconducting phase. Moreover, the spectrum of Fermi excitations has six Dirac points, the existence of which is a well-known starting point for finding the Majorana fermions [11].

This work was supported by the Russian Foundation for Basic Research, project nos. 13-02-00523 and 14-02-31237.

REFERENCES

1. K. Takada, H. Sakurai, E. Takayama-Muromachi, F. Izumi, R. A. Dilanian, and T. Sasaki, *Nature* **422**, 53 (2003).
2. G.-Q. Zheng, K. Matano, R. L. Meng, J. Cmaidalka, and C. W. Chu, *J. Phys.: Condens. Matter* **18**, L63 (2006).
3. A. Kanigel, A. Keren, L. Patlagan, K. B. Chshka, and P. King, *Phys. Rev. Lett.* **92**, 257007 (2004).
4. H. D. Yang, J.-Y. Lin, C. P. Sun, Y. C. Kang, C. L. Huang, K. Takada, T. Sasaki, H. Sakurai, and E. Takayama-Muromachi, *Phys. Rev. B* **71**, 020504R (2005).
5. G.-Q. Zheng, K. Matano, D. P. Chen, and C. T. Lin, *Phys. Rev. B* **73**, 180503R (2006).
6. G. Baskaran, *Phys. Rev. Lett.* **91**, 097003 (2003).
7. B. Kumar and B. S. Shastry, *Phys. Rev. B* **68**, 104508 (2005).
8. M. Ogata, *J. Phys. Soc. Jpn.* **72**, 1839 (2003).
9. Q.-H. Wang, D.-H. Lee, and P. A. Lee, *Phys. Rev. B* **69**, 092504 (2004).
10. S. Zhou and Z. Wang, *Phys. Rev. Lett.* **100**, 217002 (2008).
11. Y.-M. Lu and Z. Wang, *Phys. Rev. Lett.* **110**, 096403 (2013).
12. R. O. Zaitsev, *Sov. Phys. JETP* **41**, 100 (1975), *Sov. Phys. JETP* **43**, 574 (1976).
13. R. O. Zaitsev, *Diagram Methods in Theory of Superconductivity and Ferromagnetism* (URSS, Moscow, 2004) [in Russian].
14. N. M. Plakida, *High-Temperature Superconductivity* (Springer, Berlin, 1995).
15. V. V. Valkov and A. A. Golovnya, *J. Exp. Theor. Phys.* **107**, 996 (2008).
16. P. W. Anderson, *Phys. Rev.* **110**, 827 (1958), *Phys. Rev.* **112**, 1900 (1958).

Translated by K. Kugel